Total Electron Content Effects on GNSS Augmentation Systems

J. A. Klobuchar[(1)], P. H. Doherty[(2)], M. Bakry El-Arini[(3)], R. Lejeune[(4)], T. Dehel[(5)]

[(1)]ISI, Inc., 27 Conant Road, Lincoln, MA 01773 U. S. A. (tecgps@aol.com)
[(2)]Boston College, 140 Commonwealth Avenue, Chestnut Hill, MA 02467-3862 U. S. A. (dohertpd@bc.edu)
[(3)]MITRE/CAASD, 7515 Colshire Drive, McLean, VA 22102 U. S. A. (bakry@mitre.org)
[(4)]As [(3)] above, but E-mail: (rlejeune@mitre.org)
[(5)]The FAA Technical Center, ACT 360, Atlantic City, NJ 08405 U. S. A. (tom.dehel@tc.faa.gov)

ABSTRACT

The Global Navigation Satellite System can have serious range accuracy limitations due to Total Electron Content in regions where absolute TEC values and spatial gradients are very high. Model studies show that specifying TEC accurately in the equatorial anomaly region may be difficult. In the CONUS the 15 July 2000 geomagnetic storm showed large spatial TEC gradients only over part of the region. WAAS correctly specified the increased Grid Ionospheric Vertical Errors, (GIVES) in the regions of the CONUS affected by the storm, with the remainder of the region still having reasonably low TEC corrections and low GIVEs.

INTRODUCTION

Space Based Augmentation Systems, (SBASs) correct for ionospheric delay by broadcasting equivalent vertical Ionospheric Grid Delays (IGDs) at 5° x 5° IGPs, from which users (e.g., single frequency SBAS receivers on aircraft) interpolate to obtain the equivalent vertical delays at each of their Ionospheric Pierce Points (IPPs). These IPP values are then converted to slant delays at each satellite IPP using a standard conversion formula [1]. IPP is defined as the intersection of the line of sight from a receiver to a satellite and an equivalent ionospheric thin shell at a height of 350 km. TEC is directly proportional to ionospheric range delay, with 6.15×10^{16} el/m^2 being equivalent to one meter of range delay at the GPS L1 frequency. This range delay correction method works well in the midlatitude regions where spatial gradients in TEC are normally small, [2], but may not provide adequate ionospheric corrections in the equatorial region, due to the very high spatial and temporal variations of TEC that typically exist in that large region of the world. Figure 1 illustrates the geographic extent of the equatorial region over South America, along with the 5° x 5° IGPs over the entire continent. Note that the country of Brazil extends more than ±15° in magnetic dip latitude either side of the magnetic equator and that numerous IGPs are required to cover the entire South American continent.

TESTING POTENTIAL SBAS PERFORMANCE OVER SOUTH AMERICA USING MODEL TEC VALUES

The LowLat model, [3], has been shown to replicate actual TEC behavior over the equatorial region, from the magnetic equator to well past the latitude of the nominal anomaly peak latitude. Therefore it was used as the model of choice, along with appropriate ExB drifts from [4], to obtain 3 dimensional electron density profiles throughout the equatorial region under various conditions of ExB drift and solar activity. Figure 2A depicts the vertical ionospheric delays for 20 LT for the LowLat model output with zero ExB drift. Note that the maximum vertical delay of 15 meters occurs over the geomagnetic equator at a longitude that corresponds to near local noon, well off the west coast of South America, and that much of South America has a vertical delay of less than 15 meters during this time. Figure 2B shows vertical ionospheric delays for an average ExB drift. The diurnal peak for this more typical ExB condition occurs at a much more easterly longitude, corresponding to a later local time. The maximum vertical delay values occur at greater than ±15° geomagnetic latitude, and are approximately 25 to 30 meters, a factor of ≈3 greater than for the no drift condition. In fact, the entire region between roughly ±30° geomagnetic latitude has larger values of vertical delay than for the no drift condition. Figure 2B also illustrates that large spatial TEC gradients may not be represented adequately by equivalent values specified only at each 5° x 5° IGP. The conditions depicted in Figures 2A and 2B are but two examples of a portion of the range of ExB effects that are seen in the equatorial region during high solar activity conditions, F10.7 = 210. The absolute TEC values certainly will be lower during solar minimum conditions, but high solar activity conditions were used in the LowLat model to examine near-worst-case conditions. The day-to-day variability of the anomaly is such that the peak can be larger or smaller, can occur at different latitudes, or even be non-existent on different days, depending on the strength of the ExB drift on any particular day, e. g., [5], [6], [7]. The equatorial region is very large, encompassing approximately 50% of the earth's surface; hence, the ExB drift, causing the equatorial "fountain" of additional electrons, has a large effect on TEC, and of course its spatial gradients, over a wide latitude region.

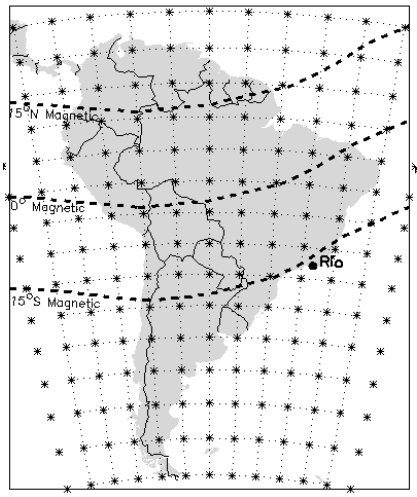

Fig. 1. Geographic extent of the equatorial region over Brazil (Units in meters)

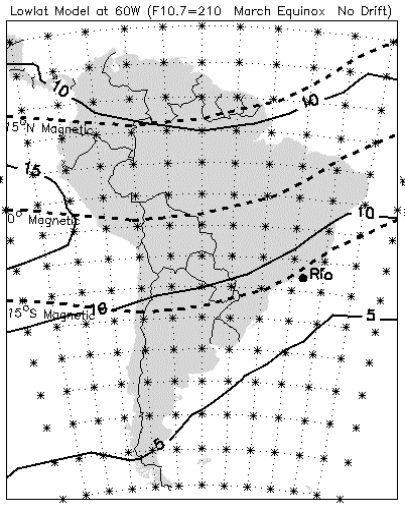

Fig. 2A. Vertical Ionospheric Range Delay for Zero ExB drift (Units in meters)

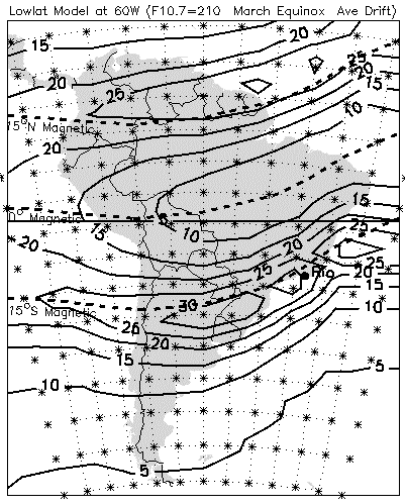

Fig. 2B. Vertical Ionospheric Range Range Delay for Average ExB drift (Units in meters)

VERTICAL DELAY ERRORS CAUSED BY THE SLANT FACTOR APPROXIMATION

For each of 104 IGP locations (from 40° S to 5° S and 30° W to 90° W), vertical delays were computed from the LowLat model for 120 lines of sight, with elevations from 5° to 75° in 5° steps, and azimuths from 0° to 315° in 45° steps, all intersecting an equivalent ionospheric thin shell at a mean height of 350 km. For each IGP the differences were computed between the vertical delay computed directly from the LowLat grid and the vertical delays obtained by projecting the slant delays computed for the 120 lines of sight along the vertical dimension, using the slant factor formula in the WAAS standard, which is the secant of the zenith angle at 350 km height. Two histograms of these slant to vertical conversion errors are shown in Figure 3 for 08 hours and 20 hours LT at 60W. These computations were made for an F10.7 value of 210. The maximum error is –13.4 m. Errors in converting between slant and vertical delays caused by the slant factor approximation are only one component of the error that a user would see when deriving the ionospheric delay along one of its lines of sight from the IGP information broadcast by an SBAS. Other errors include interpolation, estimation, and measurement errors. Interpolation errors occur when interpolating between IGDs to calculate the vertical delays at the user's IPPs. Estimation errors occur at the Master Control Station when estimating IGDs. Measurement errors result from multipath, receiver noise, and undetected cycle slips in the phase measurements.

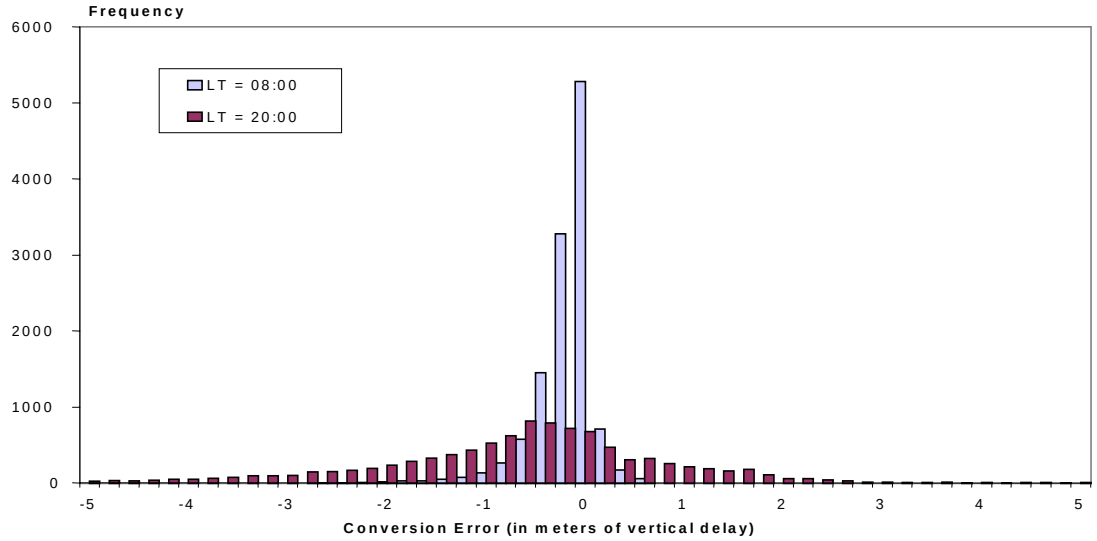

Fig. 3. Differences in vertical delay caused by the slant factor approximation.

MODEL STUDIES OF ERRORS IN 5°x 5° IONOSPHERIC GRID POINT VALUES

The present version of WAAS/SBAS is configured to specify ionospheric corrections at each 5° x 5° grid point in mid and low latitude regions (the spacing becomes 10° north of 55° N and south of 55° S). A planar surface is fitted to the vertical delays derived from the slant delay measurements located in a region around each IGP. While the planar fit is the present WAAS technique, it is not necessarily a SBAS technique. WAAS/SBAS also broadcasts residual error bounds called grid ionospheric vertical errors (GIVEs.) A measure of the quality of this procedure is the size of the residual errors from the planar fit (differences between planar and measured vertical delays) at the IPPs located within a radius of not more than 2,500 km from that IGP. Histograms of the residuals for such planar fits for the CONUS and for South American regions are shown in Figures 4A and 4B for comparison purposes. The Parameterized Ionospheric Model (PIM) was used to obtain the results shown in Fig. 4-A.

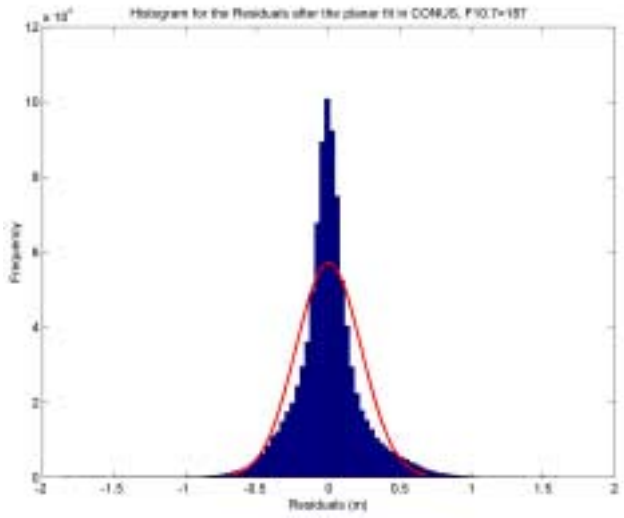

Fig. 4A. Histogram of residuals for CONUS.
(Data generated by PIM)

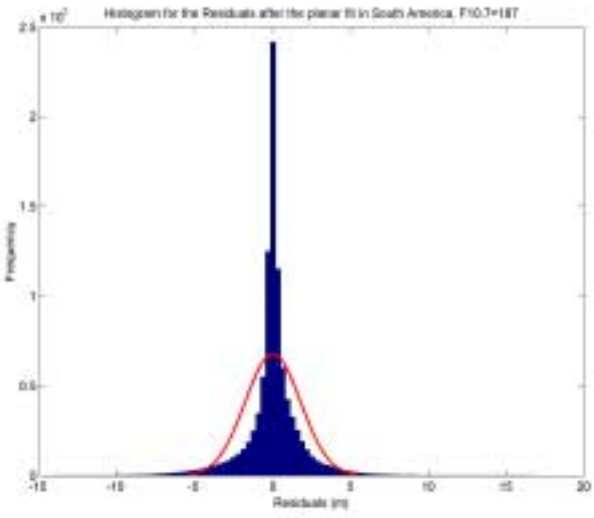

Fig. 4B. Histogram of residuals for S. A.
(Data generated by LowLat Model)

Note that the abscissa scale for Figure 4B is ten times as much as that for Figure 4A, and that the residuals for the South American Region are approximately ten times larger than for the CONUS ionosphere. The pointed shape of the distribution is also accentuated, i.e., it is moving closer to a double exponential and further away from a much more convenient Gaussian model, from a system design and safety assurance perspective.

TEC DEPLETIONS IN THE POST-SUNSET SECTOR

In addition to the large absolute TEC values and gradients that occur in the normal daytime equatorial region, during some post-sunset periods, large depletions, or "bite outs" in TEC, are seen, associated with the onset of plumes of irregularities that produce scintillation effects. These depletions can be large in absolute value, while small in geographic east-west extent. A large drop in TEC of almost 20 meters in slant TEC was observed from two stations located approximately 95 kilometers apart in an East-West direction in Brazil. These large TEC changes over small geographic regions will be difficult to observe, or represent into the standard SBAS grid, and likely will reduce system availability during post-sunset time periods that have large TEC depletions.

WAAS PERFORMANCE IN THE CONUS DURING A LARGE GEOMAGNETIC STORM

The WAAS has 21 references stations located in, or near, the CONUS, which provides an excellent opportunity to observe the performance of ionospheric range delay corrections during major geomagnetic storms. The largest storm of the present solar cycle occurred on 15 July 2000, and has been called the Saint Swithin's Day storm, while the actual solar flare that produced the storm occurred on the 14 July, and has been called the Bastille Day event. Figures 5A and 5B illustrate TEC, expressed in units of meters, across the CONUS during the late afternoon hours local time.

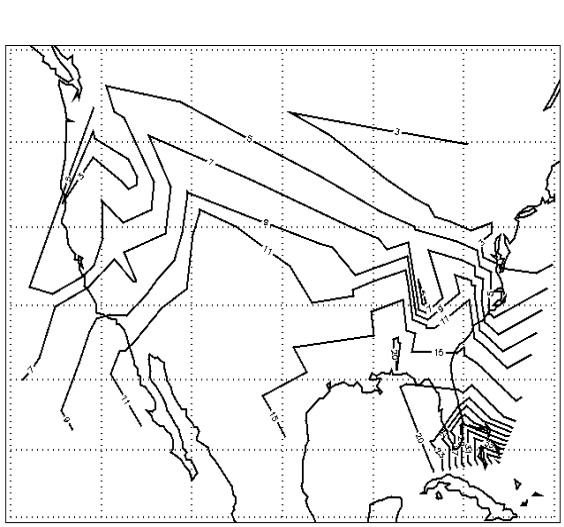

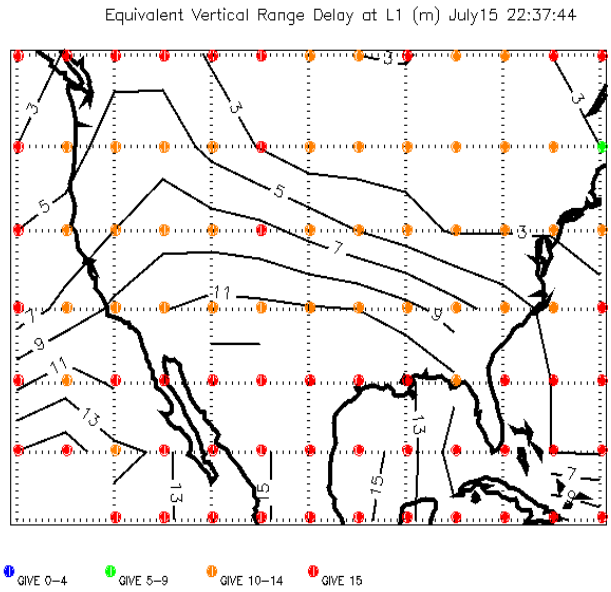

Fig. 5A. TEC contours from WAAS "SuperTruth" data, 2238 UT, 15 July 2000

Fig. 5B. TEC contours from WAAS message, 2238 UT, 15 July 2000

Note the large difference between the contours in Figure 5A and those in Figure 5B, though they are for the same time on this very disturbed day. The contours illustrated in Figure 5A were generated from actual slant TEC values from all of the WAAS reference ionospheric monitoring stations, while those in Figure 5B were generated only from the transmitted vertical 5° x 5° grid point values. Further, note that while there are large differences seen between these two representations of equivalent vertical TEC over the CONUS, the very much larger GIVEs, shown by the different colored circles in Figure 5B, clearly indicate the large gradients present during this time. The large GIVEs over the eastern and southern CONUS regions faithfully described the non-availability of WAAS ionospheric corrections during this geomagnetically disturbed time.

CONCLUSIONS

When a full constellation of dual-frequency, civilian GNSS satellite signals becomes available **all the TEC/IGD related issues will go away.** Projected plans call for a combination of the new Galileo satellites, and a later generation of GPS satellites, both to have dual-frequency signals for civilian use, to be fully in orbit sometime after the year 2010, with the potential of approximately 20 satellites in view from any station at any given time. Thus, there would be that many IPPs from which to construct ionospheric range delay values from each location. The next solar maximum will occur at nearly the same time, so the dual-frequency signals will come at an opportune time. Of course, no reasonable estimate of the magnitude of the next solar maximum is yet available, nor likely will be, until nearly that time. The issues raised in this paper open exciting areas for further research, especially in developing better methods of representing TEC in regions of the world where there are normally large temporal and spatial gradients.

References

[1] El-Arini, M. B., R. Conker, T. Albertson, J. K. Reagan, J. A. Klobuchar and P. Doherty, "Comparison of Real-time Ionospheric Algorithms for a GPS Wide-Area Augmentation System (WAAS)", Navigation, Journal of The Institute of Navigation, Vol. 41, No. 4, pp. 393-413, Winter 1994-95.

[2] Walter, T., A. Hansen, J. Blanch, P. Enge, T. Mannucci, X. Pi, L. Sparks, B. Iijima, B. El-Arini, R. Lejeune, M. Hagen, E. Altshuler, R. Fries, and A. Chu, "Robust Detection of Ionospheric Irregularities", Navigation, Journal of The Institute of Navigation, Vol., 48, No. 2, pp. 89-100, Summer 2001.

[3] Anderson, D. N., "A Theoretical Study of the Ionospheric F-Region Equatorial Anomaly, II, Results in the American and Asian Sectors, Planet. Space Sci., Vol. 21, pp. 421-442, 1973.

[4] Scherliess, L. and B.G. Fejer, "Radar and satellite global equatorial F region vertical drift model", J. Geophys. Res., Vol. 104, No. A4, pp. 6829-6842, 1999.

[5] R. G. Rastogi and J. A. Klobuchar, "Ionospheric Electron Content Within the Equatorial F2 Layer Anomaly Belt", J. Geophys. Res., Vol. 95, No. A11, pp. 19,045-19,052, Nov. 1, 1990

[6] Klobuchar, J. A., D. N. Anderson, and P. H. Doherty, "Model Studies of the Latitudinal Extent of the Equatorial Anomaly during Equinoctial Conditions", RADIO SCIENCE, Vol. 26, No. 4, pp. 1025-1047, July-August 1991.

[7] Yeh, K. C., S. J. Franke, E. S. Andreeva and V. E. Kunitsyn, "An Investigation of Motions of the Equatorial Anomaly Crest", Geophys. Res. Ltrs., Vol. 28, No. 24, pp. 4517-20, Dec. 15, 2001